University of Nebraska - Lincoln
DigitalCommons@University of Nebraska - Lincoln

Axel Enders Publications | Research Papers in Physics and Astronomy

9-1-1995

Stress evolution during the growth of ultrathin layers of iron and iron silicide on Si(111)

D. Sander
Max-Planck-Institut fu¨r Mikrostrukturphysik, Weinberg 2, 06120-Halle, Germany

Axel Enders
University of Nebraska at Lincoln, a.enders@me.com

J. Kirschner
Max-Planck-Institut fu¨r Mikrostrukturphysik, Weinberg 2, 06120-Halle, Germany

Follow this and additional works at: http://digitalcommons.unl.edu/physicsenders

 Part of the Physics Commons

Sander, D.; Enders, Axel; and Kirschner, J., "Stress evolution during the growth of ultrathin layers of iron and iron silicide on Si(111)" (1995). *Axel Enders Publications*. Paper 18.
http://digitalcommons.unl.edu/physicsenders/18

This Article is brought to you for free and open access by the Research Papers in Physics and Astronomy at DigitalCommons@University of Nebraska - Lincoln. It has been accepted for inclusion in Axel Enders Publications by an authorized administrator of DigitalCommons@University of Nebraska - Lincoln.

Stress evolution during the growth of ultrathin layers of iron and iron silicide on Si(111)

D. Sander,[a] A. Enders, and J. Kirschner
Max-Planck-Institut für Mikrostrukturphysik, Weinberg 2, 06120-Halle, Germany

(Received 4 May 1995; accepted for publication 18 July 1995)

Using a simple optical deflection technique, we measured continuously the mechanical stress during the growth of Fe films of 0.1–1.5 nm thickness on Si(111) in ultrahigh vacuum (UHV). The stress versus coverage dependence is discussed in view of the different growth modes during the various stages of Fe deposition. The deposition of up to 0.3 nm Fe induces a compressive stress of -1 N/m. We assign this stress to the formation of a reactive Fe–Si interface layer with a silicidelike structure. Subsequent Fe deposition at 300 K leads to a small tensile stress of 0.7 N/m, whereas the deposition at 600 K induces a high tensile film stress of 18 N/m. At 600 K substrate temperature, a solid-state reaction between Fe and Si sets in, and the silicide β-$FeSi_2$ is formed. The decrease of the atomic volume of Si by 7% in this silicide is proposed to be the cause for the tensile stress. © *1995 American Institute of Physics.*

A broad range of experimental techniques has been applied to examine the iron–silicon interface and the silicide film. The semiconducting β-$FeSi_2$ attracted special interest due to its reported direct energy gap of 0.89 eV.[1,2] To name a few techniques, low energy diffraction (LEED),[3–7] reflection high energy electron diffraction (RHEED)[8–11] Auger electron spectroscopy (AES) combined with electron energy loss spectroscopy (EELS),[12–16] Rutherford backscattering spectroscopy (RBS),[17] transmission electron microscopy (TEM),[18,19] photoelectron spectroscopy,[20–23] and recently scanning tunneling microscopy (STM)[24,25] experiments have been performed to characterize the structural and electronic properties of the Fe/Si system. To elucidate the issues of lattice distortion between silicon and silicide,[3,8] we measured the film stress with submonolayer sensitivity during the growth of Fe on Si at temperatures between 160 and 600 K. Our results support the more recent scenarios for the growth of Fe on Si proposed by Alvarez *et al.*,[24] favoring a reactive Fe/Si interface even at 300 K.

The experiments were carried out in an ultrahigh vacuum (UHV) chamber equipped with a Fe evaporator, Fe-flux monitor, and a quartz microbalance for calibrating the Fe-growth rates. Thus, both growth rate and film thickness were highly reproducible to within 1%. Using the magneto-optical Kerr effect (MOKE), the magnetic properties of the films could be measured *in situ*. The rectangular shaped Si(111) samples (15×5 mm^2) were cut from a double side polished wafer of 0.15 mm thickness. Samples were cleaned by heating to 1300 K under UHV conditions. Accordingly, all experiments were done on a clean Si(111)-7×7 reconstructed surface, as checked by AES and LEED. No distinct diffraction patterns were observed for the grown films. Figure 1 shows a schematic of the stress measurement setup. Details of our compact optical beam deflection technique can be found elsewhere.[26] The well-known relation[27,28] between stress σ and the experimentally determined sample curvature R was used to calculate the stress:

$$\sigma=\frac{Et_s^2}{6R(1-\nu)t_f}. \tag{1}$$

Here, the elastic properties of the sample are $E/(1-\nu)=2.2\times10^{11}$ N/m^2 for Si(111),[29] the sample thickness is given by $t_s=0.15$ mm, and t_f denotes the film thickness. The measured stress value is attributed to the homogeneously Fe-covered length of the sample, as checked by AES. An overall error bar of $\pm10\%$ must be considered for all quoted stress values, due to the uncertainties in the relevant dimensions. We prefer to speak of surface stress of the substrate, defined by $\sigma_{\mathrm{surf}}=\sigma t_f$ in units of N/m,[30,31] as the ultrathin limit, a film thickness is hard to define. Typical surface stress values are 1 N/m. Assigning this stress to a layer of 0.1 nm thickness gives a tremendous film stress of 10 GPa, which is beyond the elasticity region of steel. Nevertheless, the resulting displacement of the end of the sample amounts to only 50 nm, but this minute effect is easily detected. Even higher sensitivities can be obtained by capacitance[30–32] or more sophisticated optical methods.[33,34]

In Fig. 2 we present stress measurements for the growth of Fe on Si(111) at 300 K. The surface stress was monitored

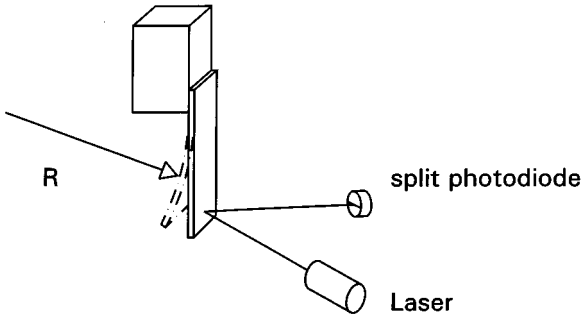

FIG. 1. The top of the sample is attached to the sample holder, the bottom end is free. The radius of curvature R of the sample is monitored by reflecting the laser beam from the sample surface to a split photodiode. Any stress on the sample surface will cause the sample to bend, thus giving rise to a position signal at the split photodiode.

[a]Electronic mail: sander@mpi-msp-halle.mpg.d

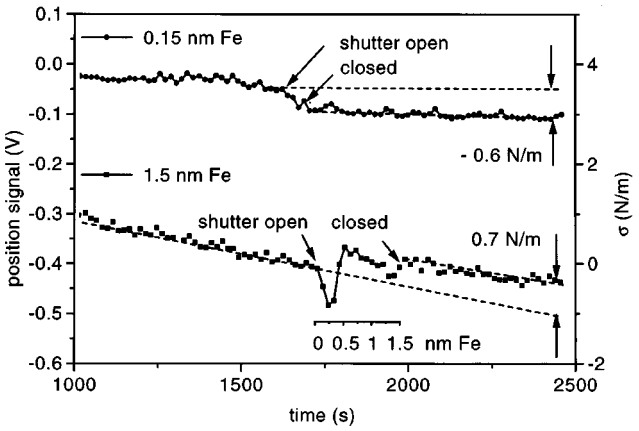

FIG. 2. Stress measurements taken during the deposition of 0.15 and 1.5 nm Fe on Si(111). The growth rate was 0.4 nm/min at T_{Si}=300 K. Stress values are obtained by measuring the offset of the position signal between the clean and the Fe-covered sample.

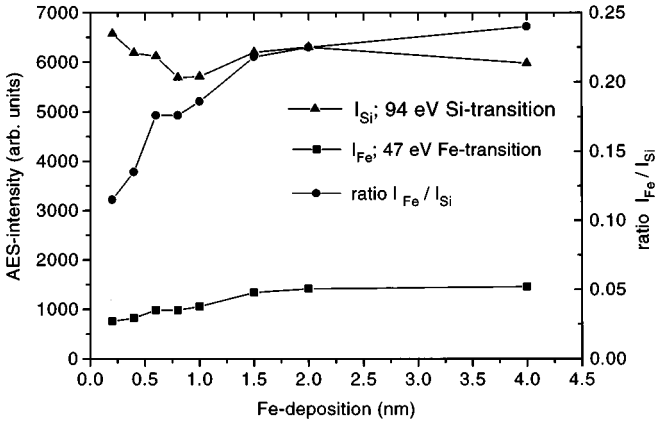

FIG. 3. Auger electron spectroscopy data taken for Fe deposition at 600 K substrate temperature. From 1.5 nm Fe deposition on, a nearly constant Auger intensity ratio of I_{Fe}/I_{Si}=0.23 is measured.

for some time and at the indicated times, the shutter of the Fe evaporator was opened. In our experiments, a negative position signal indicates a compressive stress. For the first 0.3 nm of Fe, a compressive stress of -1 N/m is measured, as shown in the lower curve in Fig. 2. For increasing Fe coverages, a tensile stress sets in that compensates for the initial compressive stress. Further deposition of Fe up to 1.5 nm creates a very small tensile stress of 0.7 N/m. Note the top curve in Fig. 2. Here, for a small deposition of up to 0.15 nm Fe, a compressive stress of -0.6 N/m is measured. We propose the formation of an intermixed Fe–Si layer to be responsible for the compressive stress. Our LEED experiments showed a strongly increased background intensity with weak 1×1 spots, even for small Fe coverages. The absence of the distinct diffraction pattern is in line with a surface reaction which destroys the long-range periodicity by creating FeSi-like patches on the surface. As our measurement of 0.15 nm Fe deposition shows, the compressive stress is maintained in the surface unless more than 0.3 nm of Fe is deposited. We conclude that there must be a change in the growth mode from 0.3 nm Fe thickness on. Comparing our results to a recent STM, UPS, ISS study by Alvarez *et al.*,[24] the compressive stress regime can be attributed to the creation of the reactive Fe–Si interface, while the tensile stress regime is attributed to the growth of Fe islands on top of this FeSi-like layer. The formation of a FeSi- or Fe_3Si-like interfacial layer is a plausible explanation for the compressive stress, as in both compounds, the atomic volume per Si atom is considerably increased.[35,36] Surplus Si atoms are forced out of their regular lattice positions in new interstitial or surface positions.[24] The so-called interstitials might play a significant role at the silicide formation at 600 K (Ref. 36), which will be discussed below.

We assign the tensile stress for Fe coverages above 0.3 nm, to the growth of $3d$-Fe-crystallites on top of this amorphous interface. This growth mode is in keeping with our AES investigations at 300 K and is known to cause tensile stress, as a result of the merging of grain boundaries.[32] In addition, further tensile contributions to the stress might be expected from comparing the interatomic distances in Fe to the values in a silicide. For all silicides, the interatomic distances are larger than for pure Fe.[35] Thus, even for $3d$-growth, we expect some tensile stress directly at the Fe-silicide interface.

At the 600 K substrate temperature, a solid-state reaction between the Fe film and Si-substrate sets in *during* deposition. The most obvious proof for this *reactive deposition epitaxy* is obtained by doing an AES-intensity study of the Fe 47 eV and the Si 94 eV peaks. In Fig. 3 we present the Fe, Si, and the Fe/Si intensity ratio as a function of Fe thickness. From our data, a Fe/Si ratio of $\sim$0.23 is extracted. This Fe/Si intensity ratio is characteristic of a $FeSi_2$ stoichiometry using our AES data. Furthermore, under these growth conditions the formation of $FeSi_2$ has been reported by Gallego and Miranda.[14] As our silicide films do not show any ferromagnetic behavior, as checked by *in situ* magneto-optical Kerr effect measurements, we exclude the formation of the magnetic γ $FeSi_2$.[9] This leaves the semiconducting β-$FeSi_2$ as the phase formed. We obtain the same AES signal ratio after annealing a 4 nm Fe layer, deposited at 160 or 300 K, for 20 min at 600 K. This silicide formation at a rather low temperature indicates the high mobility of Si in the deposited Fe film. Lau *et al.*[37] have shown that Si is the moving species during the formation of the Fe silicide.

In Fig. 4, we present data on the stress caused by the silicide formation at 600 K. To elucidate the kinetic parameters, growth rates of 0.4 and 0.1 nm/min were used. The *interface formation* during the first 0.3 nm of Fe deposition is characterized by a compressive stress, as discussed above for growth at 300 K. In contrast to the experiments done at 300 K, further Fe deposition at 600 K leads to the formation of β-$FeSi_2$ on top of this interface layer. *During* the silicide formation we measure a huge tensile stress of 11.2 and 18 N/m for the high and low growth rates, respectively.

We suggest a qualitative explanation for the tensile stress in the formed β-$FeSi_2$ layer based on the decreased atomic volume of Si[35,38] in this silicide film. Thus, as a net effect of the silicide formation, each Si atom occupies 18.7 $Å^3$ instead of 20.07 $Å^3$, thereby inducing a tensile film stress. The Fe atoms do not enter this simplified picture, as we assume that

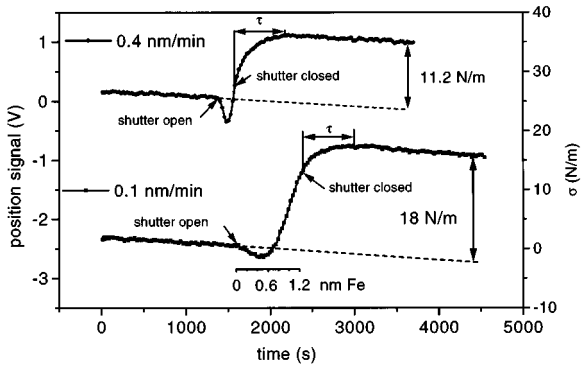

FIG. 4. Stress measurements taken during the silicide formation. Fe was deposited on a Si(111) sample heated to 600 K. For fast and slow growth rates, the same amount of time τ passes, until the stress vs time curve returns to the thermal drift line.

the arriving Fe atoms are more or less directly bonded in Fe-silicide positions. The abundancy of Si atoms at the film surface,[14] even during growth, ensures this bonding mechanism. In addition to the Si interstitials created right at the interface during the early stages of growth,[36] further *easy-diffusion channels* are likely to be formed by stress induced lattice defects in the silicide film or in the silicon substrate. Thus, an abundant supply of Si atoms seems plausible. As we measure stress *during a reactive* deposition of Fe, our results cannot be explained by an existing stress model.[39] In contrast to our experiments, this model, as most stress measurements do,[39] start from a metal-Si compound, which reacts to form a silicide.

From the stress versus time plots in Fig. 4 some important facts on the kinetics and relaxation processes of the silicide formation can be learned. At the higher growth rate, the stress continues to increase rapidly for the first 60 s after the shutter has been closed, whereas as the lower growth rate, the stress increase slows down at the moment the flux of Fe is terminated. We suggest that at the higher growth rate the flux of Si atoms to the surface is not sufficient to create the energetically favorable $FeSi_2$ stoichiometry instantaneously. The unreacted Fe undergoes its transition to $FeSi_2$ during the first 60 s after completion of the Fe deposition. A further contribution to the stress increase, valid for both rates, is assigned to a structural reorientation, that might be driven by achieving a local β-$FeSi_2$ structure as perfect as possible. The lower final stress of 11.2 N/m measured for growth at higher rates compared to 18 N/m measured at the lower rate indicates an incomplete reaction of the Fe atoms for deposition at higher rates.

In conclusion, our stress measurements clearly show, how different growth modes and solid-state reactions can be identified by a characteristic stress behavior. Thus, stress measurements contribute important information on the atomistic processes at interfaces and thin films.

[1] M. I. Bost and J. E. Mahan, J. Appl. Phys. **58**, 2696 (1985).
[2] M. I. Bost and J. E. Mahan, J. Appl. Phys. **64**, 2034 (1988).
[3] D. R. Peale, R. Haight, and J. Ott, Appl. Phys. Lett. **62**, 1402 (1993).
[4] T. Urano and T. Kanaji, Appl. Surf. Sci. **33/34**, 68 (1988).
[5] F. Scarinci, S. Lagomarsino, C. Giannini, G. Savelli, P. Castrucci, A. Rodia, and L. Scopa, Appl. Surf. Sci. **56–58**, 444 (1992).
[6] S. Kennou, N. Cherief, R. C. Cinti, and T. A. Nguyen Tan, Surf. Sci. **211/212**, 685 (1989).
[7] J. W. Ridgway and D. Haneman, Surf. Sci. **24**, 451 (1971).
[8] J. Derrien, J. Chevrier, V. Le Thanh, and J. E. Mahan, Appl. Surf. Sci. **56–58**, 382 (1992).
[9] N. Onda, J. Henz, E Müller, K. A. Mäder, and H. von Känel, Appl. Surf. Sci. **56–58**, 421 (1992).
[10] J. Chevrier, V. Le Thanh, S. Nitsche, and J. Derrien, Appl. Surf. Sci. **56–58**, 438 (1992).
[11] J. E. Mahan, K. M. Geib, G. Y. Robinson, R. G. Long, Y. Xinghua, G. Bai, M. A. Nicolet, and M. Nathan, Appl. Phys. Lett. **56**, 2126 (1990).
[12] H. Moritz, B. Rösen, S. Popovic', A. Rizzi, and H. Lüth, J. Vac. Sci. Technol. B **10**, 1704 (1992).
[13] X. Wallart, H. S. Zeng, J. P. Nys, and G. Dalmai, Appl. Surf. Sci. **56–58**, 427 (1992).
[14] J. M. Gallego and R. Miranda, J. Appl. Phys. **69**, 1377 (1991).
[15] A. Rizzi, H. Moritz, and H. Lüth, J. Vac. Sci. Technol. A **9**, 912 (1991).
[16] Q. G. Zhu, H. Iwasaki, E. D. Williams, and R. L. Park, J. Appl. Phys. **60**, 2629 (1986).
[17] C. Schwarz, N. Onda, S. Goncalves-Conto, H. Sirringhaus, and H. von Känel, J. Appl. Phys. **76**, 7256 (1994).
[18] X. W. Lin, M. Behar, J. Desimoni, H. Bernas, J. Washburn, and Z. Liliental-Weber, Appl. Phys. Lett. **63**, 105 (1993).
[19] N. Cherief, C. D'Anterroches, R. C. Cinti, T. A. Nguyen Tan, and J. Derrien, Appl. Phys. Lett. **55**, 1671 (1989).
[20] J. Alvarez, J. J. Hinarejos, E. G. Michel, and R. Miranda, Surf. Sci. **287/288**, 490 (1993).
[21] J. M. Gallego, J. M. Garcia, J. Alvarez, and R. Miranda, Phys. Rev. B **46**, 13339 (1992).
[22] J. Alvarez, J. J. Hinarejos, E. G. Michel, G. R. Castro, and R. Miranda, Phys. Rev. B **45**, 14042 (1992).
[23] M. D. DeCrescenzi, G. Gaggiotti, N. Motta, F. Patella, F. Balzarotti, and J. Derrien, Phys. Rev. B **42**, 5871 (1990).
[24] J. Alvarez, A. L. Vazquez de Parga, J. J. Hinarejos, J. De La Figuera, E. G. Michel, C. Ocal, and R. Miranda, Phys. Rev. B **47**, 16048 (1993).
[25] A. L. Vazquez de Parga, J. De La Figuera, C. Ocal, and R. Miranda, Europhys. Lett. **18**, 595 (1992).
[26] D. Sander, A. Enders, and J. Kirschner, Ref. Sci. Instrum. (to be published).
[27] A. Brenner and S. Senderoff, J. Res. Natl. Bur. Stand. **42**, 105 (1949).
[28] G. G. Stoney, Proc. R. Soc. London Ser. A **82**, 172 (1909).
[29] W. A. Brantley, J. Appl. Phys. **44**, 534 (1972).
[30] D. Sander and H. Ibach, Phys. Rev. B **43**, 4263 (1991).
[31] D. Sander, U. Linke, and H. Ibach, Surf. Sci. **272**, 318 (1992).
[32] R. Koch, J. Phys. Condens. Matter. **6**, 9519 (1994).
[33] A. J. Shell-Sorokin and R. M. Tromp, Phys. Rev. Lett. **64**, 1039 (1990).
[34] R. E. Martinez, W. A. Augustyniak, and J. A. Golovchenko, Phys. Rev. Lett. **64**, 1035 (1990).
[35] B. Eggert and G. Panzner, Phys. Rev. B **29**, 2091 (1984).
[36] M. Ronay and R. G. Schad, Phys. Rev. Lett. **64**, 2042 (1990).
[37] S. S. Lau, J. S.-Y. Feng, J. O. Olowolafe, and M.-A. Nicolet, Thin Solid Films **25**, 415 (1975).
[38] Y. Dusausoy, J. Protas, R. Wandji, and B. Roques, Acta Crystallogr. Sect. B **27**, 1209 (1971).
[39] S.-L. Zhang and F. M. d'Heurle, Thin Solid Films **213**, 34 (1992).